

Original Article

Ivermectin inhibits tumor metastasis by regulating the Wnt/ β -catenin/integrin β 1/FAK signaling pathway

Lu Jiang^{1,3}, Ying-Jian Sun², Xiao-Hua Song¹, Yan-Yan Sun¹, Wen-Yao Yang¹, Jing Li¹, Yi-Jun Wu¹

¹Laboratory of Molecular Toxicology, Institute of Zoology, State Key Laboratory of Integrated Management of Pest Insects and Rodents, Chinese Academy of Sciences, Beijing 100101, China; ²Department of Veterinary Medicine, Beijing University of Agriculture, Beijing 102206, China; ³Henan University of Chinese Medicine, Zhengzhou 450046, Henan, China

Received May 7, 2022; Accepted September 1, 2022; Epub October 15, 2022; Published October 30, 2022

Abstract: Tumor metastasis is the major cause of cancer mortality; therefore, it is imperative to discover effective therapeutic drugs for anti-metastasis therapy. In the current study, we investigated whether ivermectin (IVM), an FDA-approved antiparasitic drug, could prevent cancer metastasis. Colorectal and breast cancer cell lines and a cancer cell-derived xenograft tumor metastasis model were used to investigate the anti-metastasis effect of IVM. Our results showed that IVM significantly inhibited the motility of cancer cells *in vitro* and tumor metastasis *in vivo*. Mechanistically, IVM suppressed the expressions of the migration-related proteins via inhibiting the activation of Wnt/ β -catenin/integrin β 1/FAK and the downstream signaling cascades. Our findings indicated that IVM was capable of suppressing tumor metastasis, which provided the rationale on exploring the potential clinical application of IVM in the prevention and treatment of cancer metastasis.

Keywords: Cancer metastasis, Wnt/ β -catenin/integrin β 1/FAK, xenograft model, avermectin, colorectal cancer, breast cancer, HCT-8, anti-metastasis

Introduction

Cancer cells are highly prone to metastasis during the process of tumorigenesis and progression. They can break away from primary sites and colonize and propagate in other parts of the body, leading to the impaired function of essential organs and body system [1-3]. The process of tumor metastasis is complex, which is influenced by many factors, including epithelial-mesenchymal transitions (EMT) which is the process of epithelial cells transforming into the mesenchymal cells with high migration and invasion ability [4, 5], tumor microenvironment [6], intercellular communication [7], cells and extracellular matrix interaction [8-11], cell polarity, cytoskeleton plasticity [12, 13], and colonization of the cancer cells in the target tissues [14]. However, the effective clinical strategies to control tumor metastasis are still limited.

Several signaling pathways are involved in tumor metastasis by regulating one or more steps of the process [15-18]. For example, Wnt/ β -catenin and integrin β 1/FAK signaling

pathways play crucial roles in tumor metastasis [19, 20] by regulating EMT [21], activating paxillin, and enhancing the expression of Rho GTPase family proteins [22]. Accordingly, some drugs or plant extracts have been reported to regulate metastasis through modulating their activity [23-27].

Ivermectin (IVM), a derivative of avermectin B1, belongs to the class of 16-membered macrolide compounds, and has been widely used to treat parasites, pest insects, and vectors of diseases [28-31]. Importantly, two macrolide compounds, abamectin and doramectin, have been reported to inhibit the expression of cytoskeletal proteins in mouse neuroblastoma N2a cells [32]. Furthermore, studies have shown that both IVM and selamectin, an avermectin monosaccharide analogue, inhibit the migration of breast cancer MDA-MB-231 cells *in vitro*, and selamectin inhibits the lung metastasis of mouse 4T1 breast cancer cells *in vivo* [33]. Based on these findings, we speculated that IVM might have inhibitory effect on the motility of cancer cells.

Ivermectin inhibits tumor metastasis by Wnt signaling pathway

In this study, we investigated the effect of IVM on cell migration and tumor metastasis. By using multiple tumor cell lines and xenograft tumor models [34, 35], we not only revealed the inhibition of IVM on tumor metastasis, but also identified novel molecular mechanisms mediating the inhibitory effect of IVM on the motility of cancer cells.

Materials and methods

Cell culture

The human colorectal cancer HCT-8 cell line and breast cancer MCF-7 cell line were obtained from Shanghai Huiying Biological Technology Co. Ltd (Shanghai, China). The human colorectal cancer HCT-116 cell line and breast cancer MDA-MB-231 cell line were from Nanjing KeyGen Biotech Inc. (Jiangsu, China). EGFR-knockout HCT-116 cell line [36] was kindly provided by Dr. Ningzhi Xu at Chinese Academy of Medical Sciences (Beijing, China). All cells were cultured in RPMI-1640 medium (Sigma-Aldrich), supplemented with 10% FBS at 37°C in a humidified atmosphere of 5% CO₂.

Chemicals and reagents

Ivermectin (purity > 95%) was purchased from Dalian Meilun Biological Technology Co. Ltd (Liaolin, China). Vincristine sulphate (purity ≥ 96.7%) was purchased from Wuhan Yuancheng Gongchuang Technology Co. Ltd (Hubei, China). Adriamycin was purchased from KeyGen Biotech (Jiangsu, China). CK1 activator pyrvinium pamoate [6-(dimethylamino)-2-[2-(2,5-dimethyl-1-phenylpyrrol-3-yl) ethenyl]-1-methyl-quolinium; PP] was purchased from Sigma-Aldrich (St Louis, MO, USA). Millicell hanging cell culture inserts were purchased from EMD Millipore Corporation (Billerica, MA, USA). Matrigel was purchased from Corning Incorporated (Bedford, MA, USA). Recombinant human Wnt3a protein were purchased from R&D Systems (Minneapolis, MN, USA). Antibodies against GSK3β (#9832), p-GSK3β^{ser9} (#5558), β-catenin (#8480), p-β-catenin (#9561), LRP6 (#2560), p-LRP6 (#2568), frizzled5 (#5266), Histone H3 (#4499), E-cadherin (#5296), Rac1/Cdc42 (#4651), vimentin (#3932), FAK (#3285), p-FAK (#3283), Paxillin (#2542), p-Paxillin (#2541), and snail (#3879) were purchased from Cell Signaling Technology (Boston, MA, USA); antibodies for TCF4 (ab217668), integrin β1 (ab-

52971), and MMP9 (ab38898) were obtained from Abcam (Cambridge, UK); antibodies against RhoA, Rac1, and Cdc42 were purchased from Cytoskeleton (Denver, CO, USA); antibodies to detect ZO-1 (339100) and occludin (331500) from Life Technologies Corporation (Carlsbad, CA, USA); antibodies against Tubulin (sc20852) and GAPDH (CW0100) were purchased from Santa Cruz Biotechnology (Santa Cruz, CA, USA) and CoWin Biotechnology (Beijing, China), respectively.

Xenograft tumor models and IVM treatment

Four-week-old male non-obese diabetic/severe combined immune deficient (NOD/SCID) mice (Vital River) were used in our *in vivo* assay to test the effect of IVM on tumor progression and metastasis. Mice were fed with standard rodent chow and water ad libitum and were housed 5 mice per cage on individually ventilated caging racks.

To establish the xenograft colorectal carcinoma model, 100 μl of 1 × 10⁷ HCT-8 cells were subcutaneously inoculated into the flank region of mice. Tumor growth was monitored, and when tumor size reached about 100 mm³, the mice were randomized into three groups (n = 3/group). The IVM solution (in 0.9% NaCl) was injected intraperitoneally daily at the doses of 0, 2, and 3 mg/kg/day, respectively, for 18 days. Injection of 0.9% NaCl solution was used as vehicle control. Tumors sizes were measured every three days using calipers, and tumor volume was calculated as V = length × width²/2. At the end of the treatment, tumors were dissected and weighed.

To establish the colorectal carcinoma metastasis model, intravenous tail vein injection of 100 μl of 2 × 10⁶ HCT-8 cells were performed, and the mice were randomized into four groups (n = 6/group). For IVM treatment groups, the IVM solution was injected intraperitoneally daily at the doses of 0, 1, 2, and 3 mg/kg/day, respectively, for 37 days. Injection of 0.9% NaCl solution was served as vehicle control. At the end of the treatment, tumor nodules were dissected and fixed in 4% paraformaldehyde for histological examination.

All animal studies were performed in accordance with the guidance of Chinese legislation, and the animal protocol was reviewed and approved by the Animal and Medical Ethics

Ivermectin inhibits tumor metastasis by Wnt signaling pathway

Committee of the Institute of Zoology, Chinese Academy of Sciences.

RhoA/Rac1/Cdc42 activation assay

The cells at about 30% confluence were treated with IVM and/or VCR for 20 min and lysed to collect supernatants by centrifugation. The supernatants were then incubated with 30 μ l of RhoA activation assay beads (Rhotekin-RBD) or 10 μ l of Rac1 and Cdc42 activation assay beads (PAK-PBD) provided by Combo RhoA/Rac1/Cdc42 activation assay Biochem Kit (Cytoskeleton, Denver, CO, USA) at 4°C in rotation for 1 h. The binding complex was retrieved by centrifugation, washed once, and the precipitated beads were resuspended in 40 μ l of 2 × loading buffer for the Western blotting analysis.

Luciferase reporter assay

A 2,200 bp promoter fragment encompassing the TCF4 binding site and the annotated transcription start site of integrin β 1 gene [-2000 to +200 bp, chr10: 32958145-32960365 (hg38)] was cloned into a Gaussia luciferase (GLuc) reporter vector (pEZX-PG04, GeneCopoeia), which contains secreted embryonic alkaline phosphatase (SeAP) for transfection normalization.

The cells in 24-well plates were co-transfected with the above reporter vector and pcDNA3.1(+)-TCF4 or pcDNA3.1(+)- β -catenin expression vector using transfection reagent VigoFect. At 12 h after transfection, the cells were treated as indicated for 48 h. The activities of GLuc and SeAP were quantified with the Secrete-Pair™ dual luminescence assay kit (GeneCopoeia).

Immunofluorescence analysis

Cells were fixed in 4% paraformaldehyde for 15 min at room temperature (RT), permeabilized with 0.5% Triton X-100 for 10 min at RT, and blocked in TBST containing 3% BSA for 1 h at 37°C before incubation with antibodies against β -catenin, E-cadherin, ZO-1, and occludin at 37°C for 1.5 h. The staining signal was visualized using FITC-labeled secondary antibody for 1 h at 37°C and examined under fluorescent microscope. All images were acquired using a Carl Zeiss LSM710 laser scanning confocal microscope (Oberkochen, Germany).

Histochemistry staining

Hematoxylin and eosin staining was carried out following the standard protocol. Briefly, tissue sections were deparaffinized, rehydrated through decreasing concentration of alcohol, stained in hematoxylin for 15 min, differentiated, and then stained with eosin for 3 min followed by dehydration in alcohol and xylene. The sections were mounted and examined under Olympus IX71 inverted microscope (Tokyo, Japan).

Plasmids construction and cell transfection

DNA sequences encoding human full length β -catenin (X87838.1), TCF4 (NM_001083962.1), integrin β 1 (ITGB1 A) (NM_002211.3), and FAK (L13616.1) were cloned into mammalian expression vector pcDNA3.1(+) vector (GENEWIZ). HCT-8 cells were transfected using the transfection reagent VigoFect (Vigorous Biotech, Beijing, China).

Wound healing assay

HCT-8 cells and MCF-7 cells were grown in 24-well plates to 90% confluence. A 20 μ l-sterile tip was used for wound scratching. The cells were washed with PBS for three times and then treated as indicated in RPMI-1640 medium (containing 1% FBS). The reduction of the wound area after 24 h was visualized under the inverted microscope, quantified by CellSens standard software and compared with the same area at time 0. Percent of wound closure was the ratio between wound area at 24 h and at time 0.

Transwell assay

Transwell migration assays was conducted in 24-well chamber with 8.0 μ m pore polycarbonate membrane insert. Briefly, cells that were starved for 24 h were seeded in the upper chamber in 200 μ l of serum-free medium with or without drug treatment, while the lower chamber was filled with 20% FBS complete medium. After incubation for 48 h, the top side of upper chamber was gently swabbed with cotton-tipped applicators and the underside was fixed and stained with 0.1% crystal violet. The number of penetrating cells was determined under the inverted microscope and quantified by using ImageJ software.

Ivermectin inhibits tumor metastasis by Wnt signaling pathway

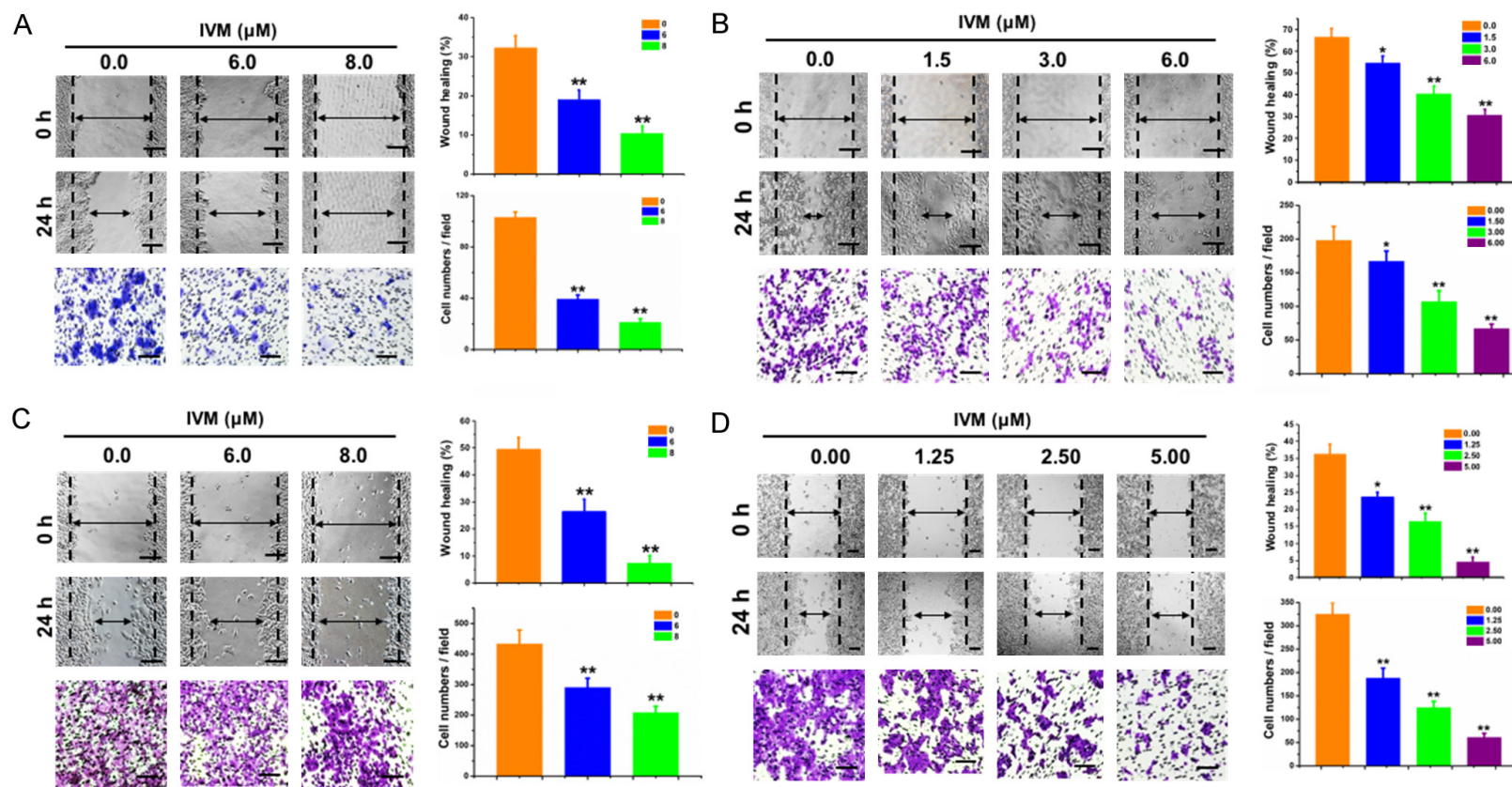


Figure 1. IVM inhibited the migration of cancer cells *in vitro*. Wound healing assay and transwell migration assay of the breast cancer MCF-7 cells (A) and MDA-MB-231 cells (B), and colorectal cancer HCT-8 cells (C) and HCT-116 cells (D). Measurement: 0, 24, and 48 h after IVM treatment, respectively. Concentrations of IVM was as indicated. Top panel: quantitation of wound closure: $([\text{distance of the wound at 0 h} - \text{distance of the wound at 24 h}] / \text{distance of the wound at 0 h} \times 100\%)$. Left bottom panel: quantitation of transwell migration assay. Scale bar = 250 μm. Cells treated with vehicle served as control. Data in the histograms were presented as the mean \pm SD (n = 3). *P < 0.05, **P < 0.01, compared with their respective controls.

Ivermectin inhibits tumor metastasis by Wnt signaling pathway

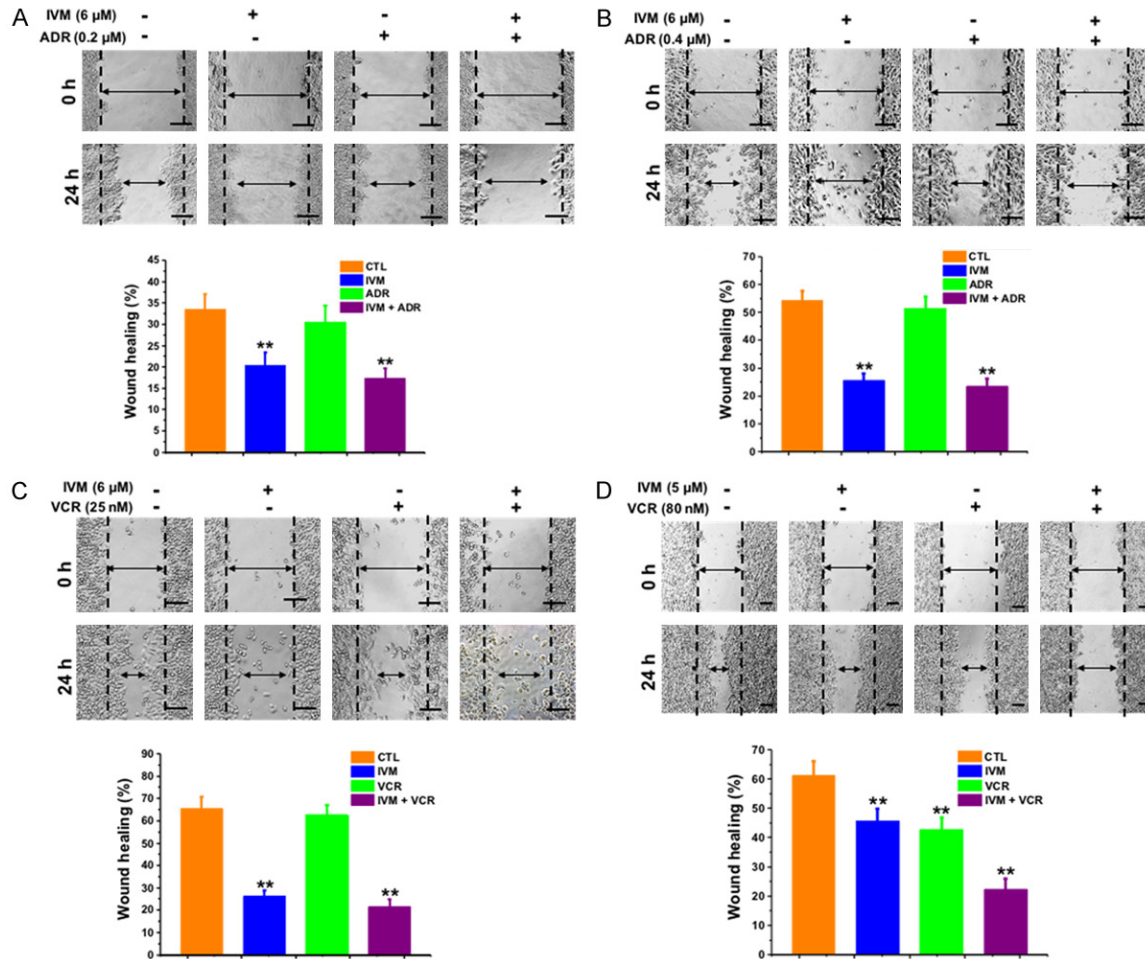


Figure 2. IVM alone or in combination with anticancer drug inhibited the migration of cancer cells *in vitro*. Breast cancer MCF-7 cells (A) and MDA-MB-231 cells (B), and colorectal cancer HCT-8 cells (C) and HCT-116 cells (D) were treated with IVM in the presence or absence of the anticancer drug adriamycin (ADR) (A and B) or vincristine (VCR) (C and D). Wound healing assay was performed at 0 and 24 h, respectively, after the treatment of IVM alone or in combination with ADR or VCR. Quantitation of wound closure was performed as described in **Figure 1**. Scale bar = 250 μm. Cells treated with vehicle served as control. Data in the histograms were presented as the mean ± SD (n = 3). **P < 0.01, compared with their respective controls.

Western blotting analysis

Briefly, cells were lysed in RIPA buffer (containing 50 mM Tris, pH 7.5, 150 mM NaCl, 1% Triton X-100, 1 mM EDTA, 1% sodium deoxycholate, 1 mM PMSF and 1% protease inhibitors), and the cells lysates were cleared by centrifugation at 5,000 g for 15 min at 4°C. The supernatants were collected, quantified, and the protein lysates were separated by SDS-PAGE. Proteins were transferred onto Millipore PVDF membranes (Darmstadt, Germany). Membranes were blocked with 5% non-fat milk or BSA in TBST buffer for 2 h at RT and then incubated with primary antibody overnight at 4°C. After

extensive washing with TBST, membranes were incubated with appropriate secondary antibody for 3 h at RT. The signal was developed by ECL reagents (Beyotime Biotechnology, Shanghai, China) and detected by DNR MicroChem4.2 system (Bio-Imaging Systems Ltd, Israel). The Western blotting images were analyzed by Quantity One software.

Cytoplasmic and nuclear protein extracts

Cells were homogenized with cytoplasmic extraction buffer (20 mM HEPES, pH 7.2, 210 mM sucrose, 70 mM mannitol, 10 mM KCl, 1 mM DTT, 1 mM EDTA, 1 mM EGTA, 1 mM PMSF and

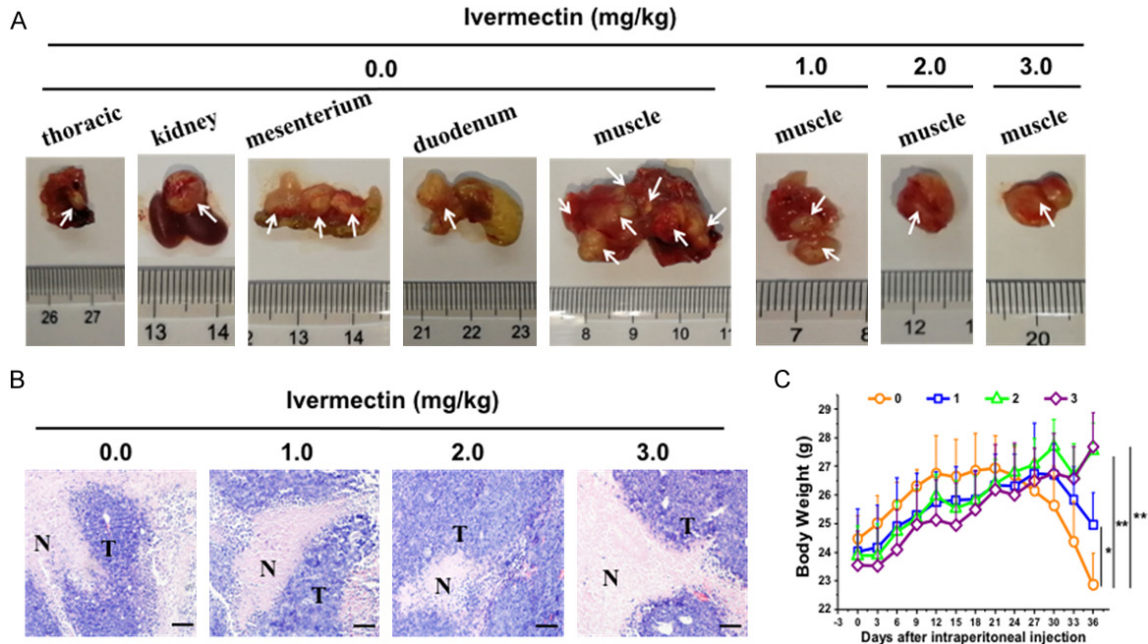


Figure 3. IVM inhibited the metastasis of HCT-8 cells-derived tumor *in vivo*. The NOD/SCID mice were injected through tail vein with 2×10^6 HCT-8 cells. The mice were then treated with different doses of IVM (0, 1, 2, or 3 mg/kg, i.p.) daily for 37 days. **A.** The mouse tissues that contained tumor nodules. White arrows indicated the metastatic tumor nodules. **B.** The histochemical examination of the tumor mass found in muscle tissue with hematoxylin and eosin staining. Scale bars = 150 μ m. N, non-tumor tissues; T, tumor tissues. **C.** The comparison of the body weight of the HCT-8 cells-inoculated mice after IVM treatment. The numbers 0, 1, 2, and 3 in the figure keys represented the IVM doses 0, 1, 2, and 3 mg/kg, respectively. Data were presented as the mean \pm SD (n = 6). *P < 0.05, **P < 0.01, compared with the vehicle controls.

Table 1. IVM inhibited the metastasis of HCT-8 cells-derived tumor *in vivo*

	Doses of (mg/kg)			
	0.0	1.0	2.0	3.0
Formation of metastasis tumors (%)	100	50	33.3	16.7
Volume of the tumor nodules (mm ³)	2410.6	730.5	249.5	125.0
Numbers of the tumor nodules	16	8	2	1
Thoracic cavity	1	0	0	0
Kidneys	1	0	0	0
Lungs	0	2	0	0
Duodenum	1	0	0	0
Mesentery	3	0	0	0
Eyes	0	1	0	0
Muscle	10	5	2	1

1% protease inhibitors) in a glass homogenizer on ice, and then was incubated for 30 min. The cells homogenates were lysed to collect supernatants as cytoplasmic extract by centrifugation at 600 g for 15 min at 4°C. Cell pellets were resuspended in the nuclear extraction buffer (50 mM Tris, pH 7.5, 150 mM NaCl, 1%

Triton X-100, 1 mM EDTA, 1% sodium deoxycholate, 1 mM PMSF and 1% protease inhibitors), sonicated for 30 s and incubated on ice for 30 min and then centrifuged at 12,000 g for 15 min at 4°C. The supernatant was collected as nuclear extract.

Chromatin immunoprecipitation assay

Chromatin immunoprecipitation (ChIP) was conducted using the EZ ChIP kit (EMD Millipore). Briefly, HCT-8 cells treated with IVM for 48 h were collected and cross-linked with formaldehyde. Chromatin was sonicated and then immunoprecipitated with TCF4, anti-RNA polymerase II (positive control), or normal rabbit IgG (negative control), respectively. The immunoprecipitated DNA fragments were detected by qPCR analysis using a TaKaRa SYBR Premix Ex Taq TM (Tli RNaseH Plus) PCR kit (Dalian, China). The primers for the integrin

Ivermectin inhibits tumor metastasis by Wnt signaling pathway

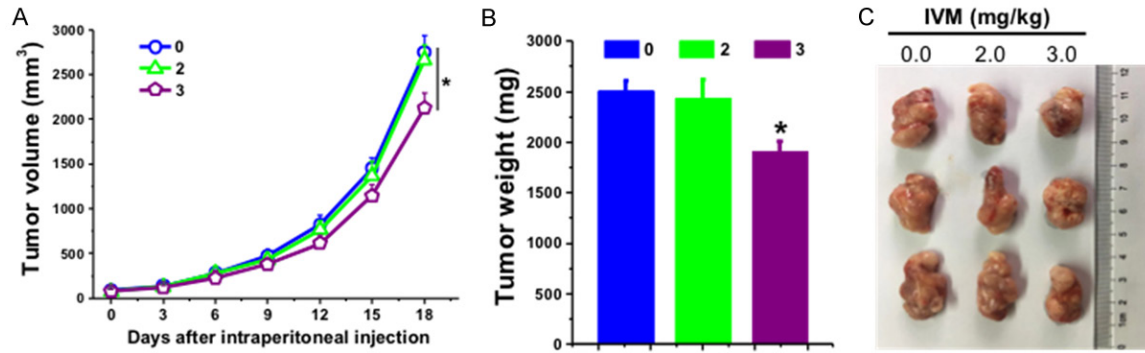


Figure 4. Effect of IVM on the growth of HCT-8 xenograft tumor *in vivo*. The NOD/SCID mice were injected subcutaneously with 1×10^7 HCT-8 cells. When the tumor reached to about 100 mm³, the mice were treated with IVM (2 or 3 mg/kg) by intraperitoneal injection daily for 18 days. (A) Tumor volumes from day 0 to day 18. (B and C) The weights (B) and images (C) of the tumors at the last day of IVM treatment. Mice treated with vehicle served as control. Data in (A and B) were presented as the mean \pm SD ($n = 3$). * $P < 0.05$, compared with the vehicle controls.

$\beta 1$ promoter (-317 to -661 bp) were 5'-TGT-TCCCATAAAGGTACCTC-3' (sense) and 5'-TTC-GACCCTCGCTCCCGTTT-3' (antisense). Quantitative PCR assay was carried out with an Axygen MX3000P real-time thermocycler (California, USA).

Statistical analysis

All experiments were repeated at least three times except that some WB experiments were repeated twice. For statistical analysis, a one-way analysis of variance (ANOVA) followed by Dunnett's test was used for multiple comparisons. Values of $P < 0.05$ were considered statistically significant, and values of $P < 0.01$ were considered extremely significant. All data were presented as mean \pm SD unless otherwise indicated.

Results

IVM inhibited the motility of multiple cancer cells *in vitro*

We first assessed the effect of IVM on the migration of MCF-7 and MDA-MB-231 cells by wound-healing assay. We found that IVM at the concentrations of 1.5-8.0 μ M markedly inhibited cell migration (Figure 1A, 1B) in a dose-dependent manner. Furthermore, the cell migration was also inhibited by IVM in combination with adriamycin (ADR), a commonly used anticancer drug, although ADR alone had minimal effect on cell migration (Figure 2A, 2B).

Consistently, IVM inhibited the migration of human colorectal cancer cell HCT-8 and HCT-

116 cells. IVM either alone or in combination with vincristine (VCR), a commonly used anti-cancer drug, inhibited the migration of HCT-8 cells, while VCR alone had no significant effect (Figures 1C and 2C). Likewise, IVM inhibited the migration of HCT-116 cells at the concentrations of 1.25-5.00 μ M in a dose-dependent manner (Figure 1D). However, different from HCT-8 cells, VCR alone could inhibit the migration of HCT-116 cells, combination of VCR and IVM further inhibited the migration of HCT-116 cells (Figure 2D).

Taken together, these cell line-based studies indicated that IVM could inhibit the migration of multiple types of cancer cells even when used in combination with anti-cancer drug.

Ivermectin inhibited the metastasis of xenograft tumor *in vivo*

To verify the *in vitro* inhibitory effect of IVM on cell metastasis, we investigated whether IVM could suppress the metastasis of cancer cells *in vivo* by using xenograft tumor model via tail vein injection of HCT-8 cells. To rule out the directly inhibitory effect of IVM on tumor growth, we also generated HCT-8 cells-derived subcutaneous tumor, and the mice received the same IVM treatment. The results showed that tail vein injection of HCT-8 cells lead to tumor metastasis in various tissues including muscle, thoracic cavity, kidneys, lungs, eyes, duodenum, and mesentery (Figure 3A and Table 1). However, IVM treatment by intraperitoneal injection significantly decrease the incidence of metastases, the volumes, and the numbers of tumor nodules, indicating that IVM could inhibit

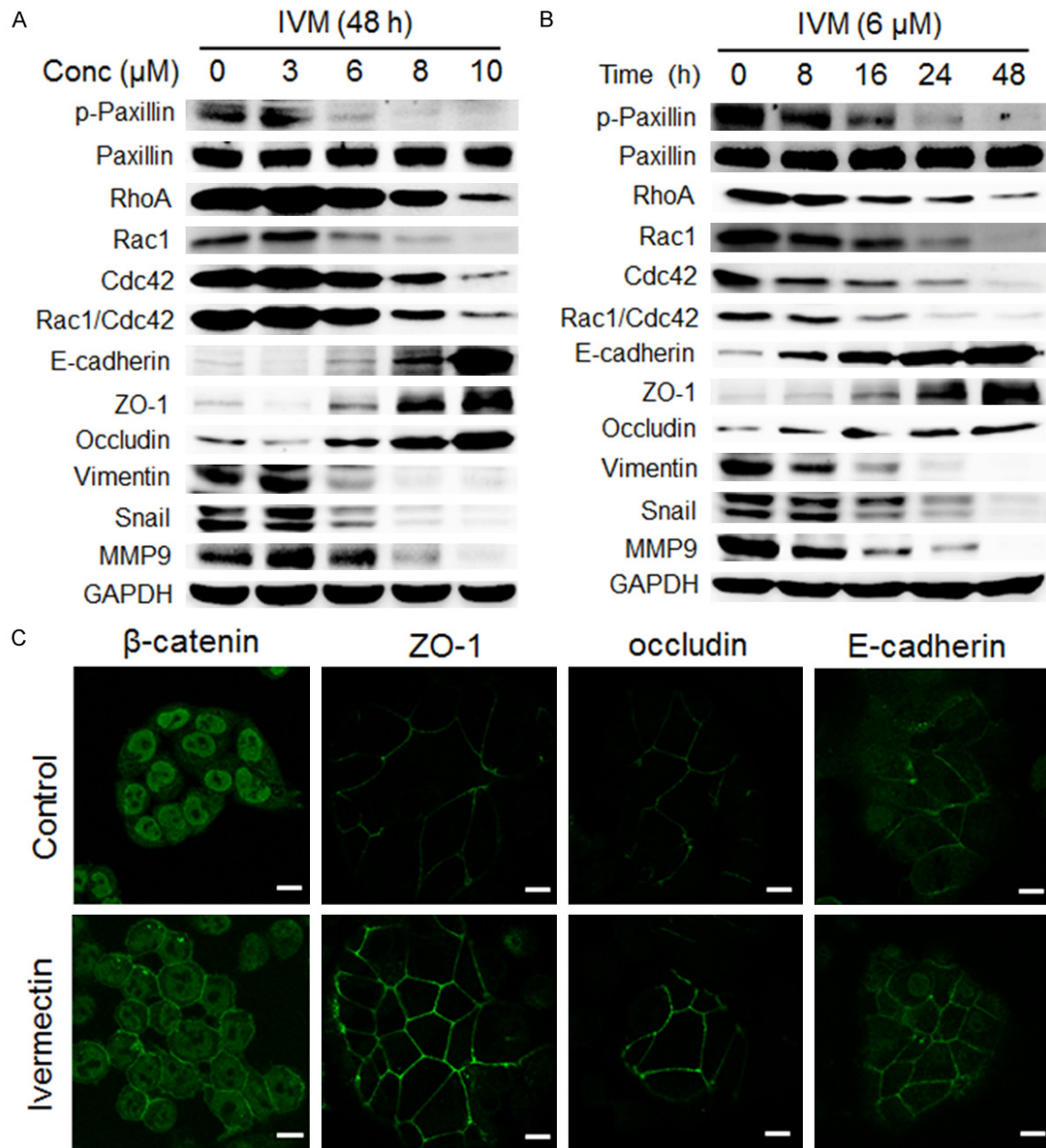


Figure 5. IVM inhibited the expressions of metastasis-related proteins in HCT-8 cells. (A and B) The expression of proteins in the cells treated with different concentrations of IVM for 48 h (A) or with 6 μM IVM for different times (B) were determined by Western blotting analysis. GAPDH was used as internal control. (C) The expression of β -catenin and epithelial cell markers ZO-1, occluding, and E-cadherin were detected in the cells by immunofluorescence analysis. Scale bars = 10 μm . Cells treated with vehicle served as control. The blots shown in (A and B) were representative of two independent experiments.

tumor metastasis in a dose-dependent manner (Table 1). The H&E staining of the extracted samples confirmed the presence of tumor mass (Figure 3B). In contrast, IVM had no obvious inhibitory effect on the growth of HCT-8 cells-derived primary subcutaneous tumor at the concentration of 2 mg/kg, while only a

slight inhibition was seen with high-dose (3 mg/kg) IVM treatment (Figure 4A-C), suggesting that IVM at the tested concentrations could inhibit the cell migration, but not the cell growth. In addition, a significant decrease in body weight was found in the vehicle-treated mice 21 days after the HCT-8 cell inoculation, while

Ivermectin inhibits tumor metastasis by Wnt signaling pathway

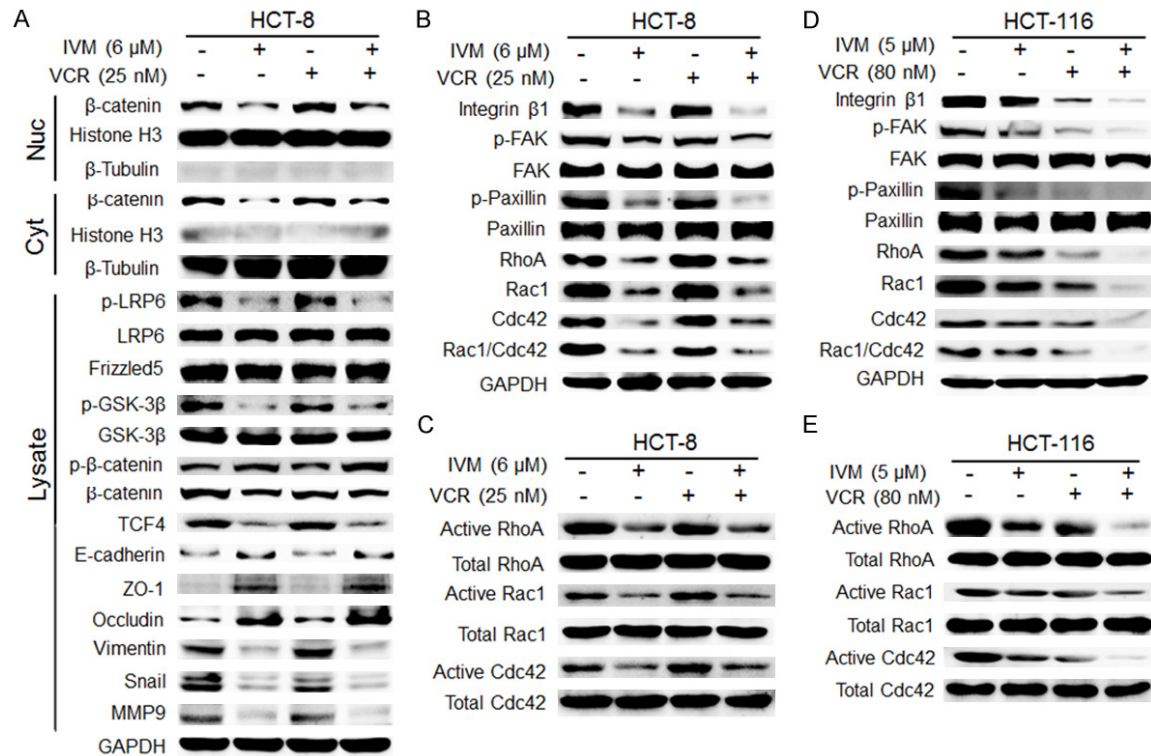


Figure 6. IVM inhibited the integrin $\beta 1$ /FAK and Wnt/ β -catenin signaling pathways in HCT-8 cells. (A) The activation of Wnt/ β -catenin pathway and the expression of the EMT-related proteins and matrix metalloproteinase-9 (MMP9) in HCT-8 cells treated with 6 μ M IVM and/or 25 nM vincristine (VCR) for 48 h were determined by Western blotting analysis using GAPDH as internal control. Histone H3 and β -tubulin were used as the nuclear and cytoplasmic fraction marker, respectively. Cells treated with vehicle served as the control. (B-E) The activation of integrin $\beta 1$ /FAK pathway and the activities of p-Paxillin, RhoA, Rac1 and Cdc42 in HCT-8 cells (B and C) and HCT-116 cells (D and E) treated with IVM and/or VCR for 48 h (B and D) or 20 min (C and E) were determined by Western blotting analysis (B and D) and pull-down assay (C and E), respectively. Abbreviations: Lysate, whole cell lysate; Nuc, nuclear lysate; Cyt, cytosolic lysate. The blots shown were representative of two independent experiments.

only a slight decrease in the low-dose (1 mg/kg) IVM-treated mice, and almost no change in the middle- and high-dose IVM-treated mice (**Figure 3C**), suggesting that IVM treatment improved the overall physical condition of tumor-bearing mice. Together, we demonstrated that IVM could inhibit the tumor metastases *in vivo*.

IVM inhibited Wnt/ β -catenin and integrin $\beta 1$ /FAK signaling pathways

Having decided the inhibitory effect of IVM on tumor metastasis, we further sought to reveal the underlying molecular mechanisms mediating IVM's activity. It has been reported that the proteins involve in intercellular junctions, cell-extracellular matrix adhesions (integrins or focal adhesions), and epithelial-mesenchymal transition (EMT) were important factors that influence cell migration [7, 8, 12, 13]. Therefore,

we first examined the effect of IVM on the expression of cell migration-related proteins in HCT-8 cells and found that IVM not only inhibited the expressions of paxillin, Rho GTPase family proteins (RhoA, Rac1, and Cdc42), mesenchymal cell markers such as vimentin and snail, and matrix metalloproteinase 9 (MMP9), but also increased the expression of epithelial cell markers such as E-cadherin, ZO-1, and occludin in a dose- and time-dependent manner (**Figure 5A, 5B**). Immunofluorescence staining also showed that IVM enhanced the expression of the epithelial cell markers (**Figure 5C**). Collectively, these results suggested that IVM might inhibit tumor cell migration by regulating the expressions of migration-associated proteins.

It has been well known that Wnt/ β -catenin and integrin $\beta 1$ /FAK signaling pathways regulate EMT, cell-cell junctions, and cell-extracellular

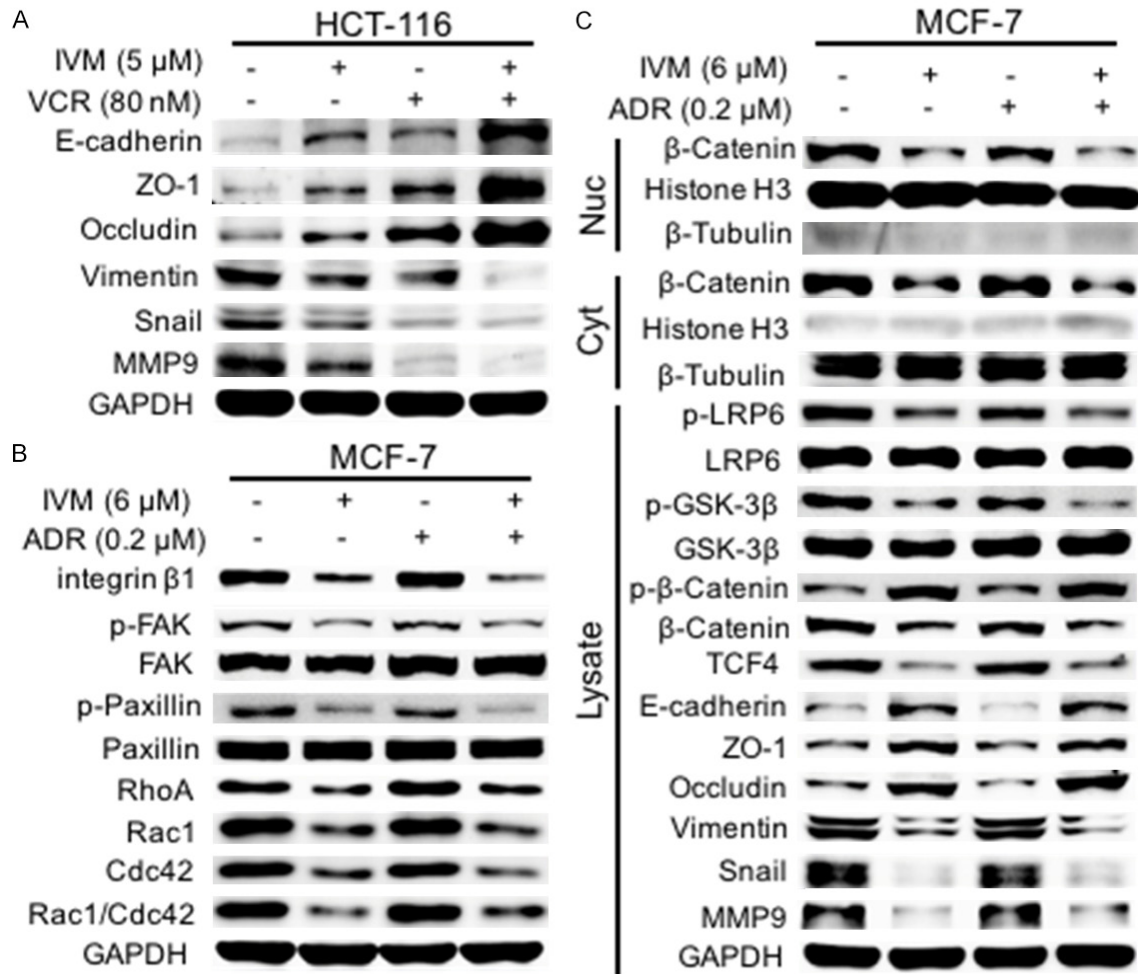


Figure 7. IVM inhibited the activation of Wnt/ β -catenin and integrin β 1/FAK pathways. (A) The expression of EMT-related proteins and MMP9 in HCT-116 cells treated with IVM and/or VCR for 48 h was determined by Western blotting analysis using GAPDH as internal control. (B and C) The activation of integrin β 1/FAK (B) and Wnt/ β -catenin (C) pathway and the expression of their downstream signaling molecules in MCF-7 cells treated with IVM and/or ADR for 48 h were determined by Western blotting analysis using GAPDH as whole cell lysate internal control. Histone H3 and β -tubulin were used as the nuclear and cytoplasmic fraction marker, respectively. Cells treated with vehicle served as the control. The blots shown were representative of two independent experiments.

matrix adhesions [21, 22]. Since immunofluorescence staining showed that IVM enhanced the localization of β -catenin on the cell membrane to maintain cell polarity (Figure 5C), we further examine the effect of IVM on Wnt/ β -catenin signaling molecules in HCT-8 cells. Our results showed that IVM not only down-regulated the level of phosphorylated LRP6 (p-LRP6), an essential co-receptor for Wnt/ β -catenin signal transduction, regardless IVM treatment alone or in combination with an anticancer drug, but also inhibited the expression of transcription factor complex β -catenin/transcription factor 4 (β -catenin/TCF4), which plays a central role in Wnt signaling pathway (Figure 6A). Moreover, IVM inhibited the activation of

integrin β 1/FAK signaling and the expressions of downstream signaling molecules p-Paxillin, RhoA, Rac1 and Cdc42 (Figure 6B). Importantly, IVM also inhibited the activation of Rho GTPase family proteins, as the levels of activated Rho, Rac and Cdc42 were lower in IVM-treated cells than in vehicle-treated cells (Figure 6C). Similar results were also observed in HCT-116 cells (Figures 6D, 6E and 7A) and MCF-7 cells (Figures 7B, 7C), suggesting the general inhibitory effect of IVM in Wnt/ β -catenin and integrin β 1/FAK signaling pathways in multiple cancer types.

To explore the relationship between Wnt/ β -catenin and integrin β 1/FAK signals during IVM-inhibited cell migration, we treated HCT-8

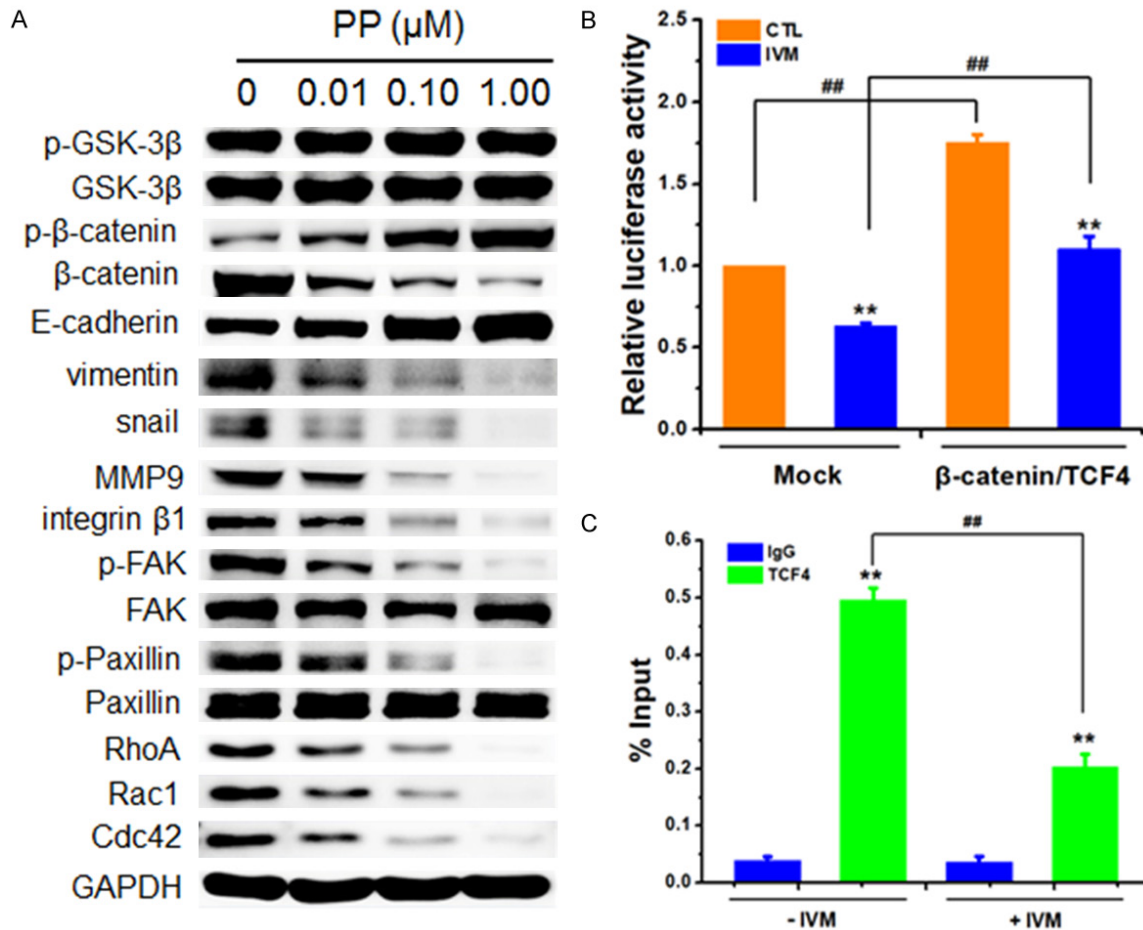


Figure 8. The Wnt/ β -catenin pathway regulated integrin β 1/FAK in HCT-8 cells. (A) The activation of Wnt/ β -catenin and integrin β 1/FAK and the expression of their downstream signaling molecules in the cells treated with different concentrations of pyrvinium pamoate (PP), an inhibitor of Wnt/ β -catenin for 48 h were determined by Western blotting analysis using GAPDH as internal control. (B) The relative integrin β 1 promoter activity of the cells co-transfected with integrin β 1 reporter plasmid, pcDNA3.1(+)-TCF4 and pcDNA3.1(+)- β -catenin plasmid and treated with 6 μ M IVM for 48 h was determined by *Gaussia* luciferase activity normalized to the activity of SeAP. (C) Chromatin IP was carried out with IgG (negative control) and anti-TCF4 antibody. Q-PCR result for integrin β 1 promoter region was shown as the percentage of input DNA. HCT-8 cells treated with vehicle or with empty vector pcDNA3.1(+) (mock) served as controls. Abbreviations: CTL, control. The blots shown in (A) were representative of two independent experiments. Data in the histograms were presented as the mean \pm SD ($n = 3$). ** $P < 0.01$, compared with their respective controls; ## $P < 0.01$.

cells with β -catenin inhibitor pyrvinium pamoate. The results showed that pyrvinium pamoate treatment decreased the expression of β -catenin, MMP9, and EMT-related proteins, suggesting that those proteins were the downstream molecules of Wnt/ β -catenin signaling. Interestingly, pyrvinium pamoate treatment also inhibited integrin β 1/FAK signaling (Figure 8A), suggesting a crosstalk between Wnt/ β -catenin signaling and integrin β 1/FAK signaling, which has not been previously reported.

To determine whether the downregulation of integrin β 1 by IVM was directly mediated by

Wnt/ β -catenin signaling transcriptional activity, we analyzed the activity of integrin β 1 promoter by co-transfecting HCT-8 cells with the reporter vector for integrin β 1 promoter and the expression vectors for β -catenin and TCF4. The luciferase reporter assay showed that the transcription factors β -catenin/TCF4 could regulate integrin β 1 activity and that the IVM-induced decrease of integrin β 1 promoter activity was restored when β -catenin and TCF4 were overexpressed in the cells (Figure 8B). Furthermore, we performed chromatin immunoprecipitation (ChIP) assay to determine whether TCF4 bound to the promoter of integrin β 1. The result

Ivermectin inhibits tumor metastasis by Wnt signaling pathway

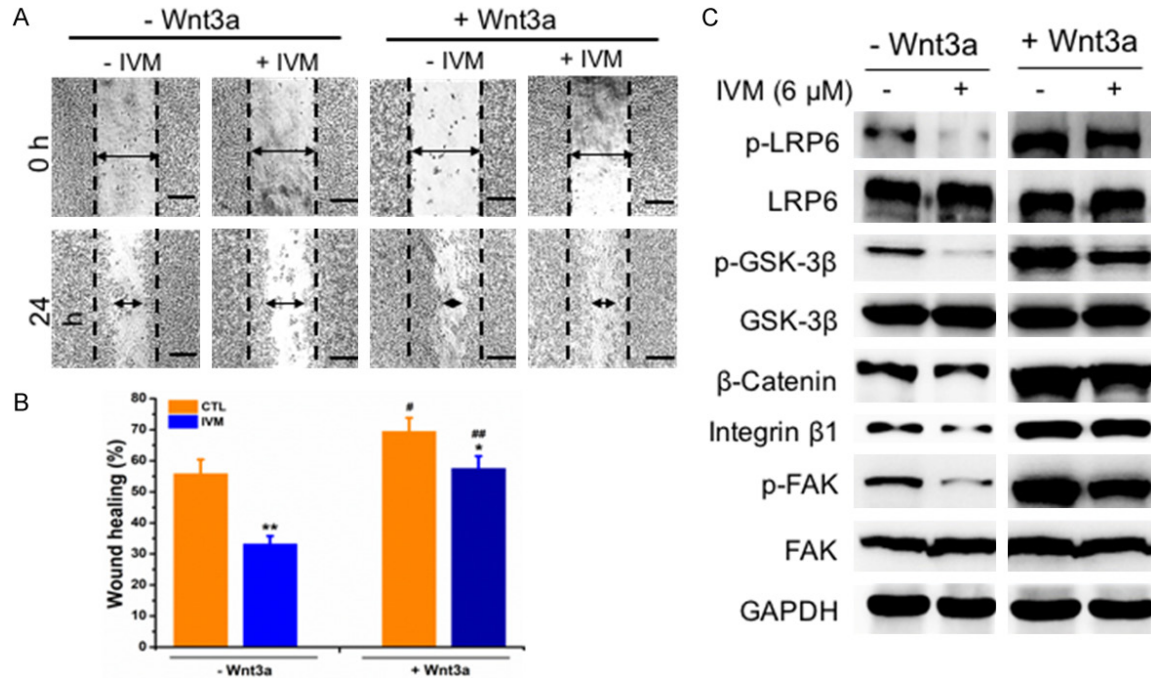


Figure 9. IVM inhibited HCT-8 cells migration through suppressing Wnt/ β -catenin/integrin β 1/FAK signaling pathway. A. Wound healing assay was carried out at 0 h and 24 h, respectively, after the cells were treated with or without 6 μ M IVM in the presence or absence of 200 ng/ml Wnt3a. Scale bar = 250 μ m. B. Quantitation of scratch assay as described in **Figure 1**. C. The activation of Wnt/ β -catenin/integrin β 1/FAK pathway and the expression of their downstream signaling molecules in the cells treated with 6 μ M IVM and/or 25 nM VCR in the presence or absence of 200 ng/ml Wnt3a for 48 h. Data in the histograms were presented as the mean \pm SD ($n = 3$). ** $P < 0.01$, compared with their respective controls; # $P < 0.05$, ## $P < 0.01$, compared with the corresponding columns with the same color.

showed that TCF4 antibody not only immunoprecipitated TCF4 proteins but also could pull down the integrin β 1 promoter region, and IVM treatment decreased the binding of TCF4 to the integrin β 1 promoter region (**Figure 8C**). Taken together, these data indicated that Wnt/ β -catenin signaling pathway regulated integrin β 1/FAK signaling, and the inhibition of integrin β 1 expression by IVM was mediated by the direct regulation of integrin β 1 transcription.

To directly determine whether the inhibitory effect of IVM on cancer cell migration was mediated by the attenuated activation Wnt/ β -catenin/integrin β 1/FAK signaling pathway, we treated HCT cells with Wnt3a, the frizzled receptor ligand that activates β -catenin-dependent signaling pathway. The results showed that IVM inhibited cell migration and reduced the expression of phosphorylated GSK-3 β , β -catenin, integrin β 1, and FAK (**Figure 9**); however, this decrease could be recovered by co-treatment with Wnt3a (**Figure 9**). In addition, the overexpression of β -catenin, integrin

β 1, or FAK could not only restore the migration inhibited by IVM (**Figure 10A-D**), but also rescue the activation of Wnt/ β -catenin/integrin β 1/FAK signaling as well as the expression of the downstream molecules inhibited by IVM treatment alone or in combination with the anti-cancer drug VCR (**Figure 11A-C**). In sum, these results indicated that the inhibition of cell motility by IVM was mediated by suppressing the expressions of metastasis-related proteins through inhibition of Wnt/ β -catenin/integrin β 1/FAK signaling pathway.

Discussion

In this study, we found that IVM, an FDA-approved anti-parasitic drug, had no obvious toxic effect on tumor cells at relative low concentrations, but inhibited the migration of multiple types of cancer cells *in vitro* and the metastasis of HCT-8 cells-derived tumor *in vivo*. This effect could be observed when IVM was used alone or in combination with antitumor drugs. Many studies have demonstrated that

Ivermectin inhibits tumor metastasis by Wnt signaling pathway

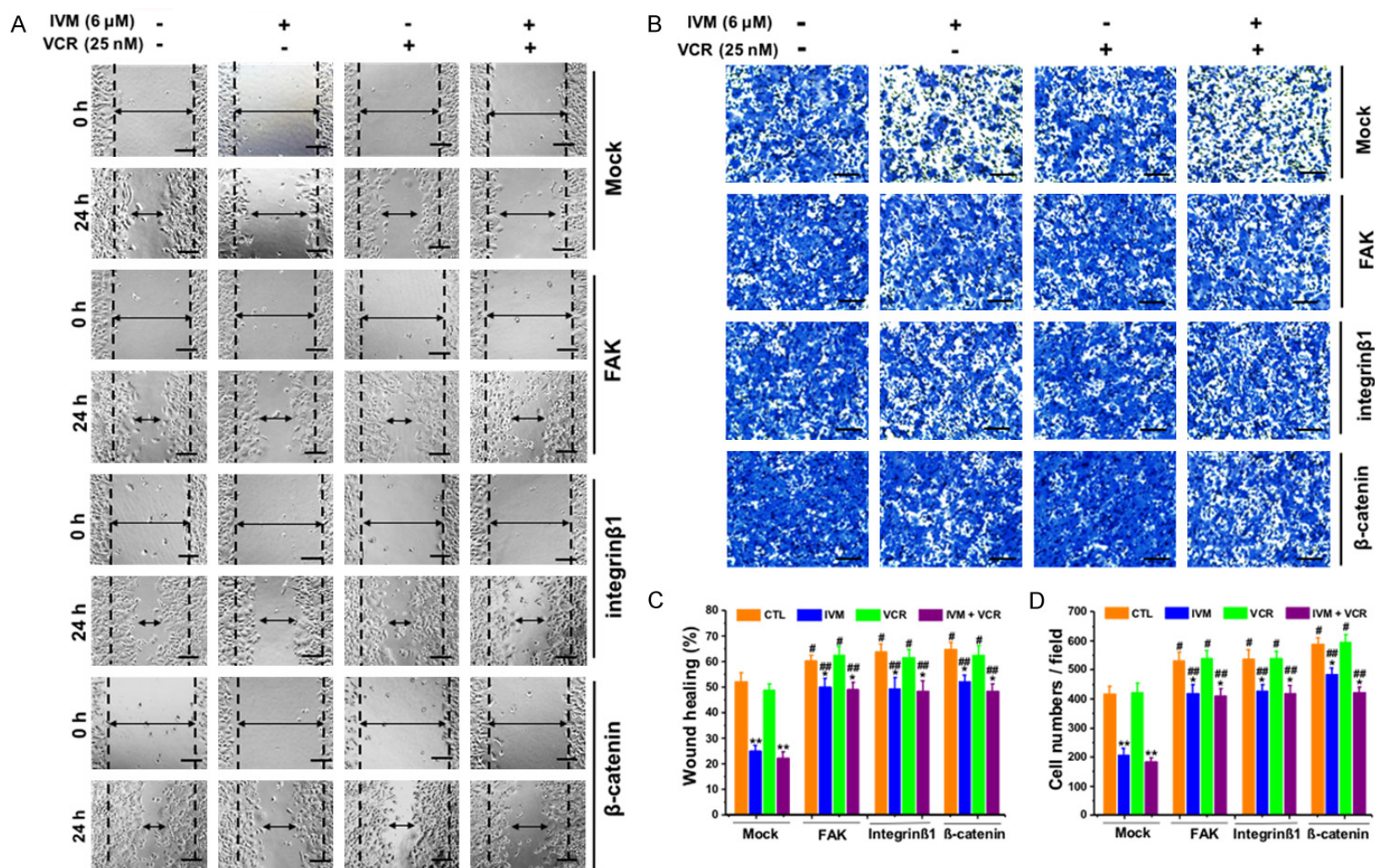


Figure 10. Overexpression of integrin β 1, FAK and β -catenin increased cell migration. (A and B) HCT-8 cell were transfected with pcDNA3.1(+)-FAK, pcDNA3.1(+)-integrin β 1, or pcDNA3.1(+)- β -catenin, and wound healing (A) and transwell migration assay (B) were assessed at 0 h and 24 h or 48 h, respectively, after treated with 6 μ M IVM and/or 25 nM VCR. Scale bar = 250 μ m. (C) Quantitation of scratch assay as described in **Figure 1**. (D) Quantitation of transwell migration assay. Cells transfected with empty vector pcDNA3.1(+) (mock) served as control. Data in the histograms were presented as the mean \pm SD (n = 3). *P < 0.05, **P < 0.01, compared with their respective controls; #P < 0.05, ##P < 0.01, compared with the corresponding columns with the same color.

Ivermectin inhibits tumor metastasis by Wnt signaling pathway

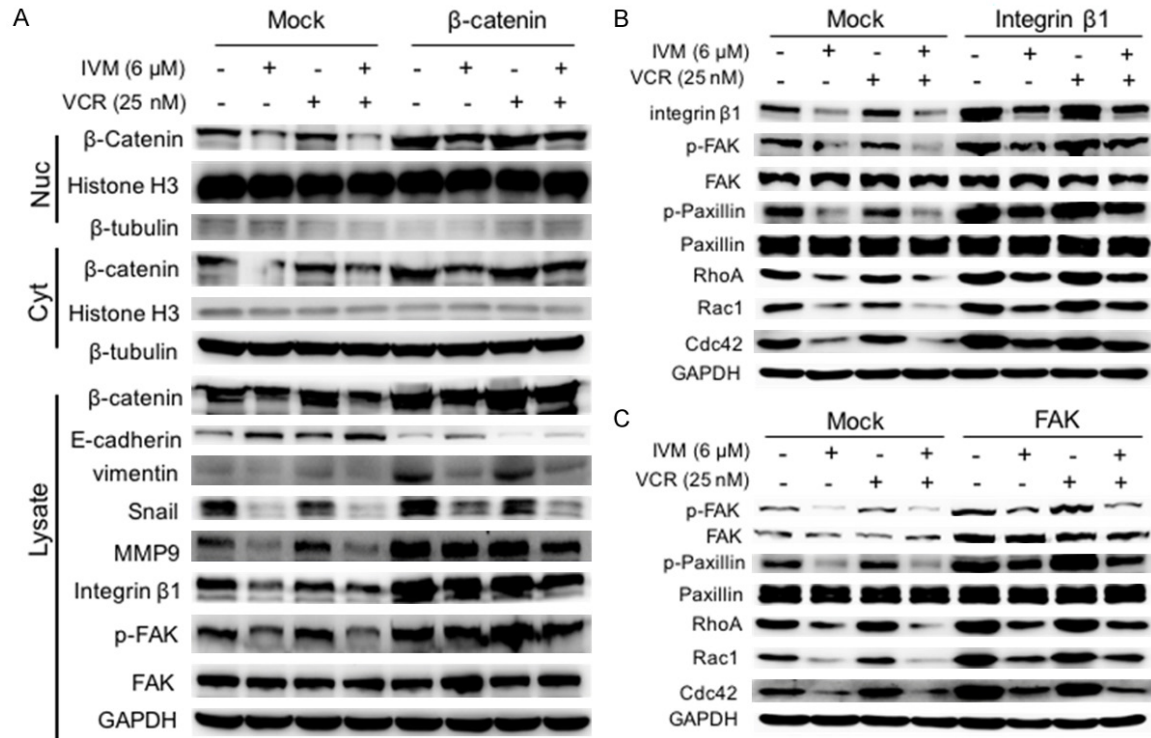


Figure 11. Overexpression of β -catenin, integrin β 1, and FAK enhanced Wnt/ β -catenin and integrin β 1/FAK signaling pathways. The activation of integrin β 1/FAK and Wnt/ β -catenin pathways, and the expression of their downstream signaling molecules in HCT-8 cells transfected with the plasmid pcDNA3.1(+)- β -catenin (A) or pcDNA3.1(+)-integrin β 1 (B), or pcDNA3.1(+)-FAK (C), and then treated with 6 μ M IVM and/or 25 nM VCR for 48 h were determined by Western blotting analysis using GAPDH as the internal control of whole cell lysate, and histone H3 and β -tubulin as the internal controls for nuclear and cytoplasmic fractions, respectively. Cells transfected with empty vector pcDNA3.1(+) (mock) served as control. The blots shown were representative of two independent experiments.

IVM caused cell death in cancer cell lines through modulating signaling pathways, including Hippo and Akt/mTOR pathways [37, 38]. It can also inhibit the growth and proliferation of cancer cells by functioning as an RNA helicase [39], or the inducer of mitochondrial dysfunction and oxidative stress [40, 41]. However, in our current study, we did not observe the IVM-inhibited cell viability and IVM-induced cell death. This discrepancy could be due to the different concentrations of IVM used in our experiments. The published studies used much higher concentrations ($> 10 \mu$ M) of IVM to observe the effect of growth inhibition and cell death induction. Additionally, the sensitivity of different cancer cell lines to IVM could be different. Nevertheless, we were the first to show that IVM inhibited cell motility and tumor metastasis at the concentration that had no effect on cell growth. Significantly, the high dose of IVM (3 mg/kg body weight) we used in the mice was equivalent to the dose used in human as

anthelmintic agent [42, 43], suggesting that the effective dose was also safe if used in clinical treatment.

Our previous studies have shown that IVM could directly interact with EGFR and inhibit EGFR signaling to suppress the growth of human cancer cells [44]. To determine whether the inhibitory effect on cell migration by IVM was also mediated by EGFR and EGFR signaling, we treated the EGFR-knockout HCT-116 cells (EGFR-KO) with IVM (Figure 12). We found that IVM also inhibited the migration of the EGFR-KO cells (Figure 12A-D), similar to that observed in wildtype HCT-116 cells (Figure 1D). IVM inhibited the activation of Wnt/ β -catenin/integrin β 1/FAK signaling pathways and the expression of the downstream signaling molecules in both EGFR-KO cells and the wildtype cells (Figure 12E), suggesting that the EGFR was not required for IVM inhibition of cell motility. Wnt/ β -catenin and integrin β 1/FAK signal-

Ivermectin inhibits tumor metastasis by Wnt signaling pathway

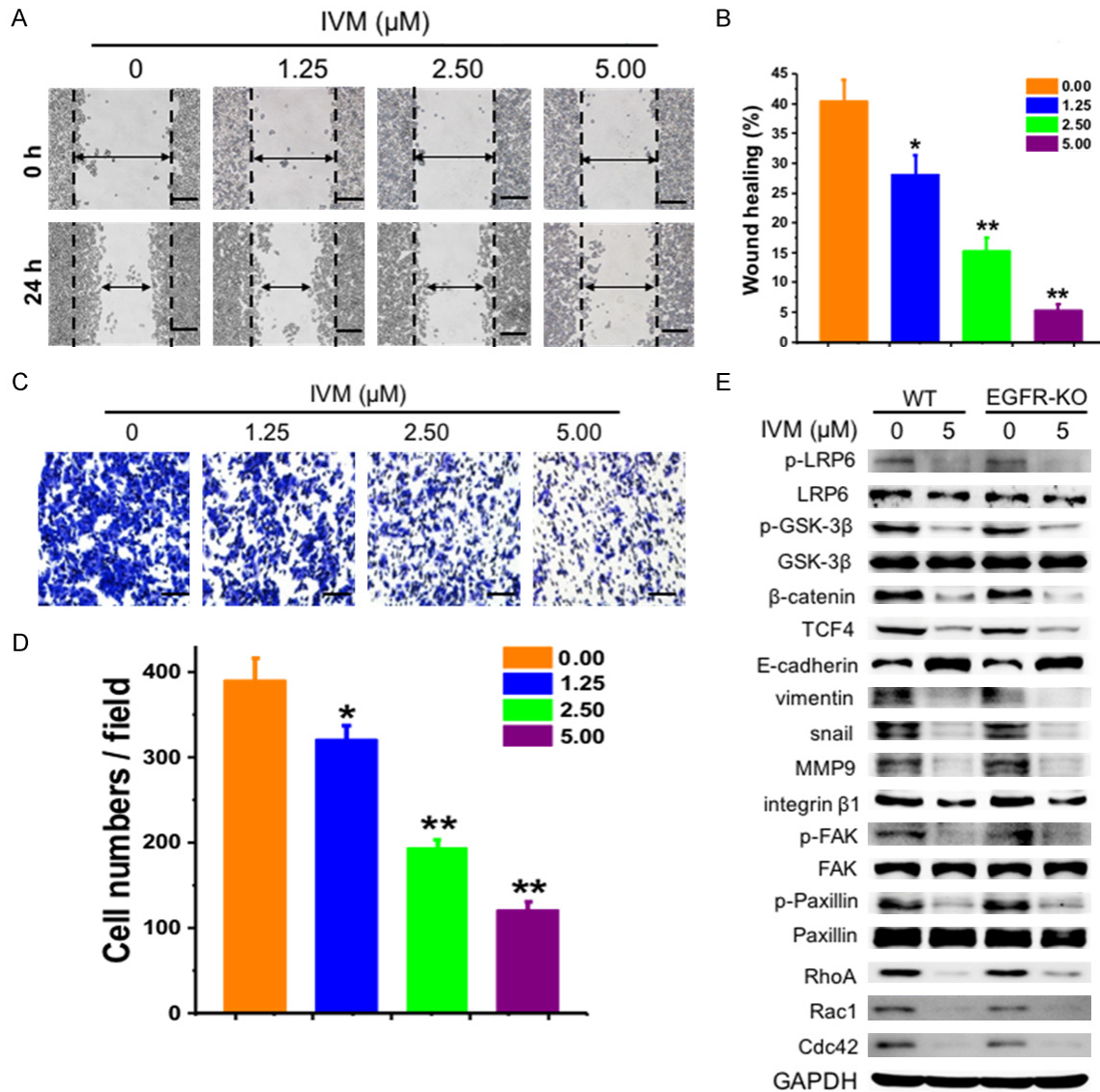


Figure 12. IVM inhibited the migration of EGFR-knockout HCT-116 cells (EGFR-KO). (A and C) Wound healing assay (A) and transwell migration assays (C) were assessed at 0 h and 24 h or 48 h, respectively, after HCT-116 EGFR-KO cells were treated with different concentrations of IVM. Scale bar = 250 μm. (B) Quantitation of scratch assay as described in **Figure 1**. (D) Quantitation of transwell migration assay. (E) The activation of integrin β1/FAK and Wnt/β-catenin pathway, and the expression of their downstream signaling molecules in HCT-116 (WT) and HCT-116 EGFR-KO cells treated with 5 μM IVM for 48 h was determined by Western blotting analysis using GAPDH as internal control. The numbers in the figure keys represented the concentrations (μM) of IVM. Cells treated with vehicle served as control. Data in the histograms were presented as the mean ± SD (n = 3). The blots shown in (E) were representative of two independent experiments. *P < 0.05, **P < 0.01, compared with their respective controls.

ing pathways have been known to play critical roles in regulating tumor metastasis [19, 20]. In our experiments, by using the inhibitors of Wnt/β-catenin and integrin β1/FAK signaling as well as overexpression of key signaling molecules in the cells, we demonstrated that IVM inhibited the cell migration by regulating the expression of the tumor metastasis-related proteins th-

rough inhibiting Wnt/β-catenin/integrin β1/FAK signaling.

Importantly, we found that the Wnt/β-catenin signaling regulated the activation of integrin β1/FAK, although it has been reported that integrin β1/FAK signaling can regulate β-catenin expression and EMT [45, 46], while Wnt/

Ivermectin inhibits tumor metastasis by Wnt signaling pathway

β -catenin signaling also regulates the activation status of integrin β 1/FAK signaling, which was consistent with our results. In addition, transcription factor complex β -catenin/TCF4 could directly regulate the transcription and expression of integrin β 1. All these results suggested the potential mechanism of IVM inhibition on cancer cell migration.

In summary, our study demonstrated that IVM could inhibit the migration of multiple types of cancer cells in vitro and the metastasis of HCT-8 cells-derived tumor in vivo. Mechanistically, IVM suppressed the expressions of metastasis-related proteins through inhibiting the Wnt/ β -catenin/integrin β 1/FAK signaling pathway. Our findings suggested that IVM could be a potential therapeutic agent for the prevention and treatment of tumor metastasis used alone or in combination with chemotherapeutic drugs.

Acknowledgements

This work was supported in part by the grant from the National Natural Science Foundation of China (No. 31672366). The authors would like to thank Mr. Ya-Nan Xu for his assistance in the animal model.

Disclosure of conflict of interest

None.

Abbreviations

AVMs, avermectins; ADR, adriamycin; ChIP, chromatin immunoprecipitation; EMT, epithelial-mesenchymal transition; FBS, fetal bovine serum; IVM, ivermectin; MMP9, matrix metalloproteinase 9; NOD/SCID, non-obese diabetic/severe combined immune deficient; VCR, vincristine; PP, pyrinium pamoate.

Address correspondence to: Yi-Jun Wu, Institute of Zoology, Chinese Academy of Sciences, Beichenxilu Rd., Chaoyang, Beijing 100101, China. Tel: +86-10-64807251; Fax: +86-10-64807099; E-mail: wuyj@ioz.ac.cn

References

[1] Pérez-González O, Cuéllar-Guzmán LF, Soliz J and Cata JP. Impact of regional anesthesia on recurrence, metastasis, and immune response in breast cancer surgery: a systematic review

of the literature. *Reg Anesth Pain Med* 2017; 42: 751-756.

- [2] Campos-da-Paz M, Dórea JG, Galdino AS, Laca-va ZGM and de Fatima Menezes Almeida Santos M. Carcinoembryonic antigen (CEA) and hepatic metastasis in colorectal cancer: update on biomarker for clinical and biotechnological approaches. *Recent Pat Biotechnol* 2018; 12: 269-279.
- [3] Zhou S, He Y, Yang S, Hu J, Zhang Q, Chen W, Xu H, Zhang H, Zhong S, Zhao J and Tang J. The regulatory roles of lncRNAs in the process of breast cancer invasion and metastasis. *Biosci Rep* 2018; 38: BSR20180772.
- [4] Termén S, Tan E, Heldin CH and Moustakas A. P53 regulates epithelial-mesenchymal transition induced by transforming growth factor. *J Cell Physiol* 2013; 228: 801-813.
- [5] Hay ED. An overview of epithelio-mesenchymal transformation. *Acta Anat (Basel)* 1995; 154: 8-20.
- [6] Zhuang X, Zhang H and Hu G. Cancer and microenvironment plasticity: double-edged swords in metastasis. *Trends Pharmacol Sci* 2019; 40: 419-429.
- [7] Tabariès S, McNulty A, Ouellet V, Annis MG, Dessureault M, Vinette M, Hachem Y, Lavoie B, Omeroglu A, Simon HG, Walsh LA, Kimbung S, Hedenfalk I and Siegel PM. Afadin cooperates with Claudin-2 to promote breast cancer metastasis. *Gene Dev* 2019; 33: 180-193.
- [8] Mitra SK and Schlaepfer DD. Integrin-regulated FAK-Src signaling in normal and cancer cells. *Curr Opin Cell Biol* 2006; 18: 516-523.
- [9] Turner CE. Paxillin interactions. *J Cell Sci* 2000; 113: 4139-4140.
- [10] Ala-aho R and Kahari VM. Collagenases in cancer. *Biochimie* 2005; 87: 273-286.
- [11] Mehner C, Hockla A, Miller E, Ran S, Radisky DC and Radisky ES. Tumor cell-produced matrix metalloproteinase 9 (MMP-9) drives malignant progression and metastasis of basal-like triple negative breast cancer. *Oncotarget* 2014; 5: 2736-2749.
- [12] Ma L, Teruya-Feldstein J and Weinberg RA. Tumour invasion and metastasis initiated by microRNA-10b in breast cancer. *Nature* 2007; 449: 682-688.
- [13] Orgaz JL, Herraiz C and Sanz-Moreno V. Rho GTPases modulate malignant transformation of tumor cells. *Small GTPases* 2014; 5: e29019.
- [14] Mahecha AM and Wang H. The influence of vascular endothelial growth factor-A and matrix metalloproteinase-2 and -9 in angiogenesis, metastasis, and prognosis of endometrial cancer. *Onco Targets Ther* 2017; 10: 4617-4624.

Ivermectin inhibits tumor metastasis by Wnt signaling pathway

- [15] Wang Y, Jing Y, Ding L, Zhang X, Song Y, Chen S, Zhao X, Huang X, Pu Y, Wang Z, Ni Y and Hu Q. Epiregulin reprograms cancer-associated fibroblasts and facilitates oral squamous cell carcinoma invasion via JAK2-STAT3 pathway. *J Exp Clin Cancer Res* 2019; 38: 274.
- [16] Yao Y, Zhou Z, Li L, Li J, Huang L, Li J, Qi C, Zheng L, Wang L and Zhang QQ. Activation of Slit2/Robo1 signaling promotes tumor metastasis in colorectal carcinoma through activation of the TGF- β /Smads pathway. *Cells* 2019; 8: 635.
- [17] Siu MKY, Jiang YX, Wang JJ, Leung THY, Han CY, Tsang BK, Cheung ANY, Ngan HYS and Chan KKL. Hexokinase 2 regulates ovarian cancer cell migration, invasion and stemness via FAK/ERK1/2/MMP9/NANOG/SOX9 signaling cascades. *Cancers (Basel)* 2019; 11: 813.
- [18] VanderVorst K, Dreyer CA, Konopelski SE, Lee H, Ho HH and Carraway KL. Wnt/PCP signaling contribution to carcinoma collective cell migration and metastasis. *Cancer Res* 2019; 79: 1719-1729.
- [19] Yang S, Liu Y, Li MY, Ng CSH, Yang SL, Wang S, Zou C, Dong Y, Du J, Long X, Liu LZ, Wan IYP, Mok T, Underwood MJ and Chen GG. FOXP3 promotes tumor growth and metastasis by activating Wnt/ β -catenin signaling pathway and EMT in non-small cell lung cancer. *Mol Cancer* 2017; 16: 124.
- [20] Wang X, Zhou Q, Yu Z, Wu X, Chen X, Li J, Li C, Yan M, Zhu Z, Liu B and Su L. Cancer-associated fibroblast-derived Lumican promotes gastric cancer progression via the integrin β 1-FAK signaling pathway. *Int J Cancer* 2017; 141: 998-1010.
- [21] Vu T and Datta PK. Regulation of EMT in colorectal cancer: a culprit in metastasis. *Cancers (Basel)* 2017; 9: 171.
- [22] Chen JY, Tang YA, Huang SM, Juan HF, Wu LW, Sun YC, Wang SC, Wu KW, Balraj G, Chang TT, Li WS, Cheng HC and Wang YC. A novel sialyltransferase inhibitor suppresses FAK/paxillin signaling and cancer angiogenesis and metastasis pathways. *Cancer Res* 2011; 71: 473-483.
- [23] Bai J and Luo X. 5-hydroxy-4'-nitro-7-propionyloxy-genistein inhibited invasion and metastasis via inactivating Wnt/ β -catenin signal pathway in human endometrial carcinoma cell endometrial cells. *Med Sci Monit* 2018; 24: 3230-3243.
- [24] Pan J, Xu Y, Song H, Zhou X, Yao Z and Ji G. Extracts of Zuo Jin Wan, a traditional Chinese medicine, phenocopies 5-HTR1D antagonist in attenuating Wnt/ β -catenin signaling in colorectal cancer cells. *BMC Complem Altern Med* 2017; 17: 506.
- [25] Shukla S, Sinha S, Khan S, Kumar S, Singh K, Mitra K, Maurya R and Meeran SM. Cucurbitacin B inhibits the stemness and metastatic abilities of NSCLC via downregulation of canonical Wnt/ β -catenin signaling axis. *Sci Rep* 2016; 6: 21860.
- [26] Li M, Yue GG, Tsui SK, Fung KP and Lau CB. Turmeric extract, with absorbable curcumin, has potent anti-metastatic effect in vitro and in vivo. *Phytomedicine* 2018; 46: 131-141.
- [27] Wang Z, Wang Y, Zhu S, Liu Y, Peng X, Zhang S, Zhang Z, Qiu Y, Jin M, Wang R, Zhong Y and Kong D. DT-13 inhibits proliferation and metastasis of human prostate cancer cells through blocking PI3K/Akt pathway. *Front Pharmacol* 2018; 9: 1450.
- [28] Williams JC, Loyacano AF, Nault C, Ramsey RT and Plue RE. Efficacy of abamectin against natural infections of gastrointestinal nematodes and lungworm of cattle with special emphasis on inhibited, early fourth stage larvae of *Ostertagia ostertagi*. *Vet Parasitol* 1992; 41: 77-84.
- [29] King CL, Suamani J, Sanuku N, Cheng YC, Sato-fan S, Mancuso B, Goss CW, Robinson LJ, Siba PM, Weil GJ and Kazura JW. A trial of a triple-drug treatment for lymphatic filariasis. *N Engl J Med* 2018; 379: 1801-1810.
- [30] Anselmi M, Buonfrate D, Guevara Espinoza A, Prandi R, Marquez M, Gobbo M, Montresor A, Albonico M, Racines Orbe M, Martin Moreira J and Bisoffi Z. Mass administration of ivermectin for the elimination of *Onchocerciasis* significantly reduced and maintained low the prevalence of *strongyloides stercoralis* in Esmeraldas, Ecuador. *PLoS Negl Trop Dis* 2015; 9: e0004150.
- [31] Pinilla YT, C P Lopes S, S Sampaio V, Andrade FS, Melo GC, Orfanó AS, Secundino NFC, Guerra MGVB, Lacerda MVG, Kobylinski KC, Escobedo-Vargas KS, López-Sifuentes VM, Stoops CA, Baldeviano GC, Tarning J, Vasquez GM, Pimenta PFP and Monteiro WM. Promising approach to reducing malaria transmission by ivermectin: sporontocidal effect against *Plasmodium vivax* in the South American vectors *Anopheles aquasalis* and *Anopheles darlingi*. *PLoS Negl Trop Dis* 2018; 12: e0006221.
- [32] Sun YJ, Long DX, Li W, Hou WY, Wu YJ and Shen JZ. Effects of avermectins on neurite outgrowth in differentiating mouse neuroblastoma N2a cells. *Toxicol Lett* 2010; 192: 206-211.
- [33] Kwon YJ, Petrie K, Leibovitch BA, Zeng L, Mezei M, Howell L, Gil V, Christova R, Bansal N, Yang S, Sharma R, Ariztia EV, Frankum J, Brough R, Sbirkov Y, Ashworth A, Lord CJ, Zelent A, Farias E, Zhou MM and Waxman S. Selective inhibition of SIN3 corepressor with avermectins as a novel therapeutic strategy in triple-negative

Ivermectin inhibits tumor metastasis by Wnt signaling pathway

- breast cancer. *Mol Cancer Ther* 2015; 14: 1824-1836.
- [34] Siegel RL, Miller KD, Fedewa SA, Ahnen DJ, Meester RGS, Barzi A and Jemal A. Colorectal cancer statistics, 2017. *CA Cancer J Clin* 2017; 67: 177-193.
- [35] McCartney A, Vignoli A, Biganzoli L, Love R, Tenori L, Luchinat C and Di Leo A. Metabolomics in breast cancer: a decade in review. *Cancer Treat Rev* 2018; 67: 88-96.
- [36] Zhang WN, Chen LC, Ma K, Zhao YH, Liu XH, Wang Y, Liu M, Liang S, Zhu H and Xu N. Polarization of macrophages in the tumor microenvironment is influenced by EGFR signaling within colon cancer cells. *Oncotarget* 2016; 7: 75366-75378.
- [37] Nishio M, Sugimachi K, Goto H, Wang J, Morikawa T, Miyachi Y, Takano Y, Hikasa H, Itoh T, Suzuki SO, Kurihara H, Aishima S, Leask A, Sasaki T, Nakano T, Nishina H, Nishikawa Y, Sekido Y, Nakao K, Shin-Ya K, Mimori K and Suzuki A. Dysregulated YAP1/TAZ and TGF- β signaling mediate hepatocarcinogenesis in Mob1a/1b-deficient mice. *Proc Natl Acad Sci U S A* 2016; 113: E71-80.
- [38] Dou Q, Chen HN, Wang K, Yuan K, Lei Y, Li K, Lan J, Chen Y, Huang Z, Xie N, Zhang L, Xiang R, Nice EC, Wei Y and Huang C. Ivermectin induces cytoskeletal autophagy by blocking the PAK1/Akt axis in breast cancer. *Cancer Res* 2016; 76: 4457-4469.
- [39] Yin J, Park G, Lee JE, Choi EY, Park JY, Kim TH, Park N, Jin X, Jung JE, Shin D, Hong JH, Kim H, Yoo H, Lee, SH, Kim YJ, Park JB and Kim JH. DEAD-box RNA helicase DDX23 modulates glioma malignancy via elevating miR-21 biogenesis. *Brain* 2015; 138: 2553-2570.
- [40] Mudassar F, Shen H, O'Neill G and Hau E. Targeting tumor hypoxia and mitochondrial metabolism with anti-parasitic drugs to improve radiation response in high-grade gliomas. *J Exp Clin Cancer Res* 2020; 39: 208.
- [41] Saied AA. Regression of bovine cutaneous papillomas via ivermectin-induced immunostimulant and oxidative stress. *J Adv Vet Anim Res* 2021; 8: 370-377.
- [42] Yang CC. Acute human toxicity of macrocyclic lactones. *Curr Pharm Biotechnol* 2012; 13: 999-1003.
- [43] Pacqué M, Muñoz B, Poetschke G, Foose J, Greene BM and Taylor HR. Pregnancy outcome after inadvertent ivermectin treatment during community-based distribution. *Lancet* 1990; 336: 1486-1489.
- [44] Jiang L, Wang P, Sun YJ and Wu YJ. Ivermectin reverses the drug resistance in cancer cells through EGFR/ERK/Akt/NF- κ B pathway. *J Exp Clin Cancer Res* 2019; 38: 265.
- [45] Gao C, Chen G, Kuan SF, Zhang DH, Schlaepfer DD and Hu J. FAK/PYK2 promotes the Wnt/ β -catenin pathway and intestinal tumorigenesis by phosphorylating GSK3 β . *Elife* 2015; 4: e10072.
- [46] Benelli R, Monteghirfo S, Venè R, Tosetti F and Ferrari N. The chemopreventive retinoid 4HPR impairs prostate cancer cell migration and invasion by interfering with FAK/AKT/GSK3 β pathway and beta-catenin stability. *Mol Cancer* 2010; 9: 142.